U.S. Department of Commerce
National Oceanic and Atmospheric Administration
National Weather Service
National Centers for Environmental Prediction
5200 Auth Road
Camp Springs, MD 20746-4304

Office Note 448

GENERALIZED EULER-MACLAURIN FORMULAE AND END CORRECTIONS FOR ACCURATE QUADRATURE ON FIBONACCI GRIDS

R. James Purser* and Richard Swinbank†

March 8, 2006

* Science Applications International Corporation, Beltsville, Maryland. e-mail: jim.purser@noaa.gov
† Met Office, Exeter, U.K. e-mail: richard.swinbank@metoffice.gov.uk

Abstract

Of the many structured grid arrangements which have been considered for climate or weather forecasting models, Fibonacci grids provide the most uniform discretizations in terms of the areal attribution of the grid nodes. Such grids are constructed by distributing points at certain uniform non-rational angular intervals along a shallow generative spiral that winds from pole to pole. A Fibonacci grid may include the poles as end points, in which case it is referred to here as the 'unstaggered' grid, or, by adjusting the grid locations along the generative spiral by one half of the standard angular increment, the grid becomes 'staggered' with respect to each pole. In the former case, the simplest and natural weighting for numerical quadratures assigns uniform weight to the interior (non-polar) nodes and one half of this weight to the poles themselves. In the latter case, all grid points are weighted equally in the simplest quadrature scheme.

However, should either of these Fibonacci grid configurations be adopted for climate or weather simulation models and the need for accurate spatial quadratures arise, then it is possible to demonstrate that the naive weightings described above do not provide the most accurate numerical results for smooth integrands, owing to subtle truncation error effects that occur at the poles. The principal errors are shown here to be exactly analogous to corresponding truncation effects that degrade the formal accuracy of trapezoidal and midpoint quadrature rules on finite line segments and whose quantification leads to the classical Euler-Maclaurin summation formulae for these quadratures. We derive the corresponding formulae for the two Fibonacci grids and show how, just as certain 'extended' trapezoidal and midpoint rules correct the principal truncation errors of quadratures along line segments by adjusting the weights assigned to the last few end points, analogous adjustments of the last few points of the two versions of the Fibonacci grid allow a corresponding correction of the truncation errors for the areal quadratures on these grids.

This approach achieves an arbitrarily high formal order of accuracy without the need for coordinate stretching or other devices that would destroy the geometrical simplicity of the Fibonacci grids. Should the Fibonacci grid system ever be adopted for climate models, the proposed quadrature refinements could supply more accurate global averages than can be obtained by simply the naive (unweighted) addition of the grid point values.

1. Introduction

Methods of finite-interval quadrature, based on orthogonal polynomials, are well-known in one dimension. They include the popular and very accurate Gauss-Legendre and Gauss-Chebyshev methods (e.g., Press et al., 1992), that require the spacing of the quadrature nodes and the quadrature weights to be non-uniform. In many applications, however, it is not possible to choose the grid points to suit the accuracy of the quadrature. Rather, we are given a grid, chosen by other considerations, and have to deal with the quadrature problem as best we can. If the spacing is uniform, and the two end points are taken to be the extreme points of this grid, then the well-known 'trapezoidal rule' (Henrici, 1964) provides a simple way of numerically

estimating the integral of a smooth function and gives a result accurate to second order in the interval width. In this method, the interior quadrature nodes are weighted by a, while the two end points are assigned weights of $a/2$, where a is the grid interval.

During the developments in classical numerical analysis that immediately followed the discovery of the calculus, it was appreciated that it was the abrupt termination of a grid, combined with the naive weighting above, that produced the principal components of truncation error. This is implicit in the asymptotic (generally non-convergent) Euler-Maclaurin summation formula:

$$\int_{z_1}^{z_2} f(z)\, dz = a \left[\frac{1}{2} f_0 + \frac{1}{2} f_n + \sum_{i=1}^{n-1} f_i \right] - \sum_{j=1}^{\infty} \frac{B_{2j} a^{2j}}{(2j)!} \left(f_n^{(2j-1)} - f_0^{(2j-1)} \right), \qquad (1.1)$$

where $a = (z_2 - z_1)/n$ is the width of the grid interval; where $f_i \equiv f(z_1 + ia)$; where $f^{(j)}$ denotes the jth derivative of the smooth function, f; and B_{2j} are the Bernoulli numbers (Abramowitz and Stegun, 1965).

Early pioneers of numerical integration realized that, by adjusting the weights near the ends of the domain, the formal order of accuracy of the quadrature of smooth functions could be increased. In a similar way, the 'midpoint rule' of quadrature, in which n points are placed at the centers of n equal grid intervals and given equal weights, achieves an accuracy to second-order in interval size, a, but can be made more accurate by suitable adjustments to these weights near the ends. Such 'extended trapezoidal rules' and 'extended midpoint rules' are derived in the next section by elementary methods and tabulated. However, the main objective of this note is to show that analogous corrections can be made to the quadrature weights of the two-dimensional 'Fibonacci grids' proposed independently for numerical weather and climate simulation by Swinbank and Purser (1999, 2005), and for a variety of physics applications by Hannay and Nye (2004).

In the case of the Fibonacci grids, which may either contain a polar 'end point' or be staggered with respect to the pole, the property of uniform linear spacing is replaced by the somewhat analogous property of essentially uniform areal density (over a disk or a sphere). Thus, the naive quadrature rules in this case are exactly analogous to those we have described for the line segment. The two-dimensionality, together with the peculiar spatial arrangement of the Fibonacci grid points, make the needed end corrections rather more difficult to define, in order to achieve a higher order of formal accuracy. However, should Fibonacci grids ever be adopted for climate models or for numerical weather prediction, the proposed refinements could supply valuable improvements in the accuracy of the computation of global averages compared to estimates obtained by a naive (unweighted) summation of grid point values.

Section 2 derives the extended quadrature rules for a uniform linear grid and examines the advantages that these formulae have in their use for the estimation of integrals of smooth functions. After a cursory review of the Fibonacci grids in section 3, we carry out analogous refinements to the quadrature weights at the ends (i.e., the poles) of these grids and verify that these adjustments are also advantageous for estimating smooth integrals. Concluding remarks are provided in section 4.

2. Extended trapezoidal and midpoint schemes

(a) *Simple derivation of the weights of the extended trapezoidal schemes*

We first consider the case where the uniform grid on a line is unstaggered with respect to any end points. For simplicity, we restrict attention to one end of the grid, and show how the summation of one-sided high-order quadrature formulae can be used to compute the end correction terms that, added to the trapezoidal quadrature weights, lead to 'extended' formulae of greater formal accuracy. Without loss of generality, assume the domain occupies the half-line $z \geq 0$ with grid points at $z_j = ja$ for integers, $j \geq 0$. Let $g_j = \int_0^{z_j} f(z)\, dz$ be the integral of a smooth function $f(z)$ from the end point to any grid point z_j. Then for an integer $n \geq 2$, there is a unique one-sided quadrature formula of the form,

$$g_j - g_{j-1} \approx a \sum_{k=0}^{n-1} A_{k,n} f_{j-1+k}, \tag{2.1}$$

which is exact for the case where f is any polynomial of degree $n-1$. The coefficients $A_{k,n}$ are those of the 'Adams-Moulton' family of implicit multistep methods (Gear 1971) and are tabulated for n up to 7 in Table 1. Clearly, the definite integral of f over the whole half-line is

TABLE 1. Adams-Moulton weights.

n	β	$\beta A_{0,n}$	$\beta A_{1,n}$	$\beta A_{2,n}$	$\beta A_{3,n}$	$\beta A_{4,n}$	$\beta A_{5,n}$	$\beta A_{6,n}$
2	2	1	1					
3	12	5	8	−1				
4	24	9	19	−5	1			
5	720	251	646	−264	106	−19		
6	1440	475	1427	−798	482	−173	27	
7	60480	19087	65112	−46461	37504	−20211	6312	−863

expressible as the sum of all the interval contributions of the form (2.1), and the corresponding quadrature weights, $Q_{j,n}$, in the approximation

$$g = \int_0^\infty f(z)\, dz \approx a \sum_{j=0}^{\infty} Q_{j,n} f_j, \tag{2.2}$$

are therefore,

$$Q_{j,n} = \sum_{k=0}^{j} A_{k,n}. \tag{2.3}$$

The case $n = 2$ simply reproduces the trapezoidal method. For $n > 2$ the sets of $n-1$ correction terms are each consistent with the generic form that is sometimes referred to as the 'Gregory' (Scheid 1968) or 'Newton-Gregory' (Butcher, 1987) formula. Expressing the approximation with $n > 2$ in the form,

$$a\left(\frac{1}{2}f_0 + \sum_{j=1}^{\infty} f_j + \sum_{j=0}^{n-2} W_{j,n} f_j\right) = \int_0^\infty f(z)\, dz + \mathcal{O}(a^{n+1}), \tag{2.4}$$

TABLE 2. CORRECTION WEIGHTS FOR THE ONE-ENDED NEWTON-GREGORY EXTENDED TRAPEZOIDAL FORMULAE FOR QUADRATURE ON A UNIFORM GRID OCCUPYING A HALF-LINE.

n	β	$\beta W_{0,n}$	$\beta W_{1,n}$	$\beta W_{2,n}$	$\beta W_{3,n}$	$\beta W_{4,n}$	$\beta W_{5,n}$
3	12	-1	1				
4	24	-3	4	-1			
5	720	-109	177	-87	19		
6	1440	-245	462	-336	146	-27	
7	60480	-11153	23719	-22742	14762	-5449	863

we may tabulate the correction weights $W_{j,n}$, consistent with the previously obtained $A_{j,n}$, in Table 2.

(*b*) *Derivation of the Euler-Maclaurin coefficients*

The derivation above, employing a summation of appropriate one-sided quadrature formulae, does not directly generalize to the Fibonacci grids of the next section. However, if we examine the moments up to degree $n-2$ of the weights, $W_{j,n}$, in Table 2, we find that they are precisely of the magnitudes required to offset the errors implied by the relevant (one-sided) part of the Euler-Maclaurin formula (1.1) at the boundary of the semi-infinite interval $[0,\infty)$. Since, as we show in the next section, the Euler-Maclaurin formula, in its special form for a half-line, *does* generalize to the case of Fibonacci grids, it is worthwhile to rederive here the two special one-sided forms of this expression that relate to quadratures on grids either unstaggered or symmetrically staggered with respect to the single boundary point $z=0$ of a half-line, $z \geq 0$. The Fourier analysis techniques that we apply to this derivation generalize fairly naturally to the two corresponding forms of the Fibonacci grid.

We shall assume that the function whose one-sided integral we wish to estimate is sufficiently smooth (or at least some adequate approximation to it is sufficiently smooth) to permit it to be expressed by a Taylor series about the end of the interval. In this case we can examine the errors in each Taylor series term one by one. The term associated with the pth derivative of the function is proportional to what we can regard as test function, z^p, for $z \geq 0$ (zero otherwise), but both the summation and the integral on the left side of (2.4) diverge for such a test function, so we must regularize the expression. We proceed by defining the Fourier transform pair:

$$f(z) = \int_{-\infty}^{\infty} \tilde{f}(k) \exp(-2\pi i k z)\, dk, \tag{2.5a}$$

$$\tilde{f}(k) = \int_{-\infty}^{\infty} f(z) \exp(+2\pi i k z)\, dz, \tag{2.5b}$$

and state the 'convolution theorem' corresponding to this transform convention:

$$\widetilde{fg} = \tilde{f} * \tilde{g}, \tag{2.6a}$$

$$\widetilde{f * g} = \tilde{f}\tilde{g}, \tag{2.6b}$$

where the convolution shorthand is defined by:

$$f * g|_z = \int_{-\infty}^{\infty} f(z-z')g(z')\, dz'. \tag{2.7}$$

Let the pair of '*comb*' functions, $C^{\pm}$ be defined as the following arrays of 'delta functions':

$$C^{+}(z) = \sum_{m=-\infty}^{\infty} \delta(z-m), \tag{2.8a}$$

$$C^{-}(z) = \sum_{m=-\infty}^{\infty} \delta(z-m-1/2). \tag{2.8b}$$

The delta function $\delta(z)$ is the distribution or 'generalized function' whose defining property is that, for an arbitrary function $f(z)$, the integral, $\int f(z)\delta(z-z')\,dz = f(z')$, that is, it simply evaluates the function f at z'. From this property, we deduce that a scaling of the coordinate transforms the delta function according to $\delta(z/a) = a\delta(z)$. The Fourier transforms of the two comb functions can be shown to be:

$$\tilde{C}^{\pm}(k) = \sum_{m=-\infty}^{\infty} (\pm)^m \delta(k-m). \tag{2.9}$$

We define a family of test functions that are powers of z modified by a decaying exponential factor involving an additional parameter $\omega > 0$:

$$f_{p,\omega}(z) = \begin{cases} 0 & : \quad z < 0, \\ z^p \exp(-\omega z) & : \quad z \geq 0, \end{cases} \tag{2.10}$$

and we refer to the pure power functions obtained in the limit, $\omega \to 0$ as simply:

$$f_p(z) \equiv \lim_{\omega \to 0} f_{p,\omega}(z). \tag{2.11}$$

The transform,

$$\tilde{f}_{p,\omega}(k) = \frac{p!}{(\omega - 2\pi i k)^{p+1}}, \tag{2.12}$$

of $f_{p,\omega}$ has a well defined limit except for the singularity at $k = 0$:

$$\tilde{f}_p(k) = \begin{cases} p!(-i)^{p+1}|2\pi k|^{-(p+1)} & : \quad k < 0, \\ p!(+i)^{p+1}|2\pi k|^{-(p+1)} & : \quad k > 0. \end{cases} \tag{2.13}$$

If we symmetrize the test functions about zero, it becomes possible to express the errors associated with numerically integrating the one-sided test function with the trapezoidal scheme (corresponding to the case C^{+}) and with the midpoint scheme (corresponding to the case C^{-}) as the whole-line integrals:

$$\mathcal{E}^{\pm}_{p,\omega}(a) = \int_{-\infty}^{\infty} (C^{\pm}(z/a) - 1)\,[f_{p,\omega}(z) + f_{p,\omega}(-z)]\,/2\,dz. \tag{2.14}$$

By a change of variables, it is easy to show that

$$\begin{aligned} \mathcal{E}^{\pm}_{p,\omega}(a) &= a^{p+1}\mathcal{E}^{\pm}_{p,\omega a}(1), \\ &\equiv a^{p+1}E^{\pm}_{p,\omega a}, \end{aligned} \tag{2.15}$$

and, since the integral of a function is its Fourier transform at $k = 0$, we deduce that

$$E^{\pm}_{p,\omega} = (\tilde{C}^{\pm} - \delta) * \Re \tilde{f}_{p,\omega}\Big|_{k=0}, \tag{2.16}$$

where $\Re$ denote the real part. Note that the delta functions at $k = 0$ cancel so that, in the limit of vanishing ω, the singularity in the transform of the test function is not sampled. Owing to the symmetries of (2.13), we obtain non-vanishing errors only in the case where p is odd, say $p = 2n - 1$, whence:

$$\begin{aligned} E^{\pm}_{2n-1} &= \lim_{\omega \to 0} E^{\pm}_{2n-1,\omega}, \\ &= \frac{2(2n-1)!(-)^n}{(2\pi)^{2n}} \sum_{m=1}^{\infty} (\pm)^m \frac{1}{m^{2n}}. \end{aligned} \tag{2.17}$$

The summations are expressible using the Riemann zeta function:

$$\sum_{m=1}^{\infty} \frac{1}{m^{2n}} \equiv \zeta(2n), \tag{2.18a}$$

$$\sum_{m=1}^{\infty} (-)^m \frac{1}{m^{2n}} \equiv -\eta(2n) \equiv -(1 - 2^{1-2n})\zeta(2n), \tag{2.18b}$$

or, equivalently, the Bernoulli numbers (Abramowitz and Stegun 1965), since:

$$(-)^{n-1}\zeta(2n) = \frac{(2\pi)^{2n}}{2(2n)!} B_{2n}. \tag{2.19}$$

Defining the limiting forms, $\mathcal{E}^{\pm}_p(a) = \lim_{\omega \to 0} \mathcal{E}^{\pm}_{p,\omega}(a)$, error coefficients consistent with the two relevant one-sided Euler-Maclaurin formulae emerge:

$$\mathcal{E}^{+}_{2n-1}(a) = -\frac{(2n-1)!}{(2n)!} B_{2n} a^{2n}, \tag{2.20a}$$

$$\mathcal{E}^{-}_{2n-1}(a) = \frac{(2n-1)!}{(2n)!} (1 - 2^{1-2n}) B_{2n} a^{2n}. \tag{2.20b}$$

Note that we can identify the factors $(2n-1)!$ with the evaluation, at $z = 0$, of the $(2n-1)$th derivative of the test function, f_{2n-1}, or other smooth test functions containing such a component among their Taylor series. A tabulation of the first few of the non-vanishing standardized coefficients, $E^{\pm}_p = \mathcal{E}^{\pm}_p(1)$, is given in Table 3.

(*c*) *Inferring correction weights of general extended quadrature from the corresponding Euler-Maclaurin coefficients*

In order to compensate for the $n - 1$ errors, up to $\mathcal{E}^{+}_{n-2}(a)$ we need a vector of correction weights, $aW_{j,n} \quad j = 0, n-2$, such that

$$\sum_{j=0}^{n-2} B_{p,j} W^{+}_{j,n} = -E^{+}_p, \qquad p = 0, \ldots n-2, \tag{2.21}$$

TABLE 3. THE FIRST FEW NON-VANISHING STANDARDIZED ERROR COEFFICIENTS FOR TRAPEZOIDAL (E^+) AND MIDPOINT (E_-) RULES.

p	β^+	$\beta^+ E_p^+$	β^-	$\beta^- E_p^-$
1	12	-1	24	1
3	120	1	960	-7
5	252	-1	8064	31
7	240	1	30720	-127

where the $B_{p,j}$ are the Vandermonde coefficients:

$$B_{p,j} = j^p. \tag{2.22}$$

It is readily verified that the coefficients of Table 2 are consistent with these prescriptions for each order of accuracy, n.

Just as the coefficients of successive rows of Table 2 can be obtained to offset the Euler-Maclaurin terms (2.20a) for all p up to degree $n-2$, we may similarly construct a table for correcting the residual errors implied by (2.20b) in the midpoint scheme. In this case, the matrices of Vandermonde coefficients, $B_{p,j+1/2}$ are used (with integer j). The resulting table of correction weights is Table 4. The extended midpoint scheme having $n-1$ correction weights is therefore:

$$a\left(\sum_{j=1}^{\infty} f_{j-\frac{1}{2}} + \sum_{j=1}^{n-1} W_{j-\frac{1}{2},n} f_{j-\frac{1}{2}}\right) = \int_0^{\infty} f(z)\,dz + \mathcal{O}(a^{n+1}). \tag{2.23}$$

TABLE 4. END CORRECTION WEIGHTS FOR THE EXTENDED MIDPOINT QUADRATURE ON A UNIFORM GRID OCCUPYING A HALF-LINE.

n	β	$\beta W_{\frac{1}{2},n}$	$\beta W_{\frac{3}{2},n}$	$\beta W_{\frac{5}{2},n}$	$\beta W_{\frac{7}{2},n}$	$\beta W_{\frac{9}{2},n}$	$\beta W_{\frac{11}{2},n}$
3	24	1	-1				
4	24	2	-3	1			
5	5760	703	-1389	909	-223		
6	5760	909	-2213	2145	-1047	206	
7	967680	184831	-532379	681550	-497086	195203	-32119

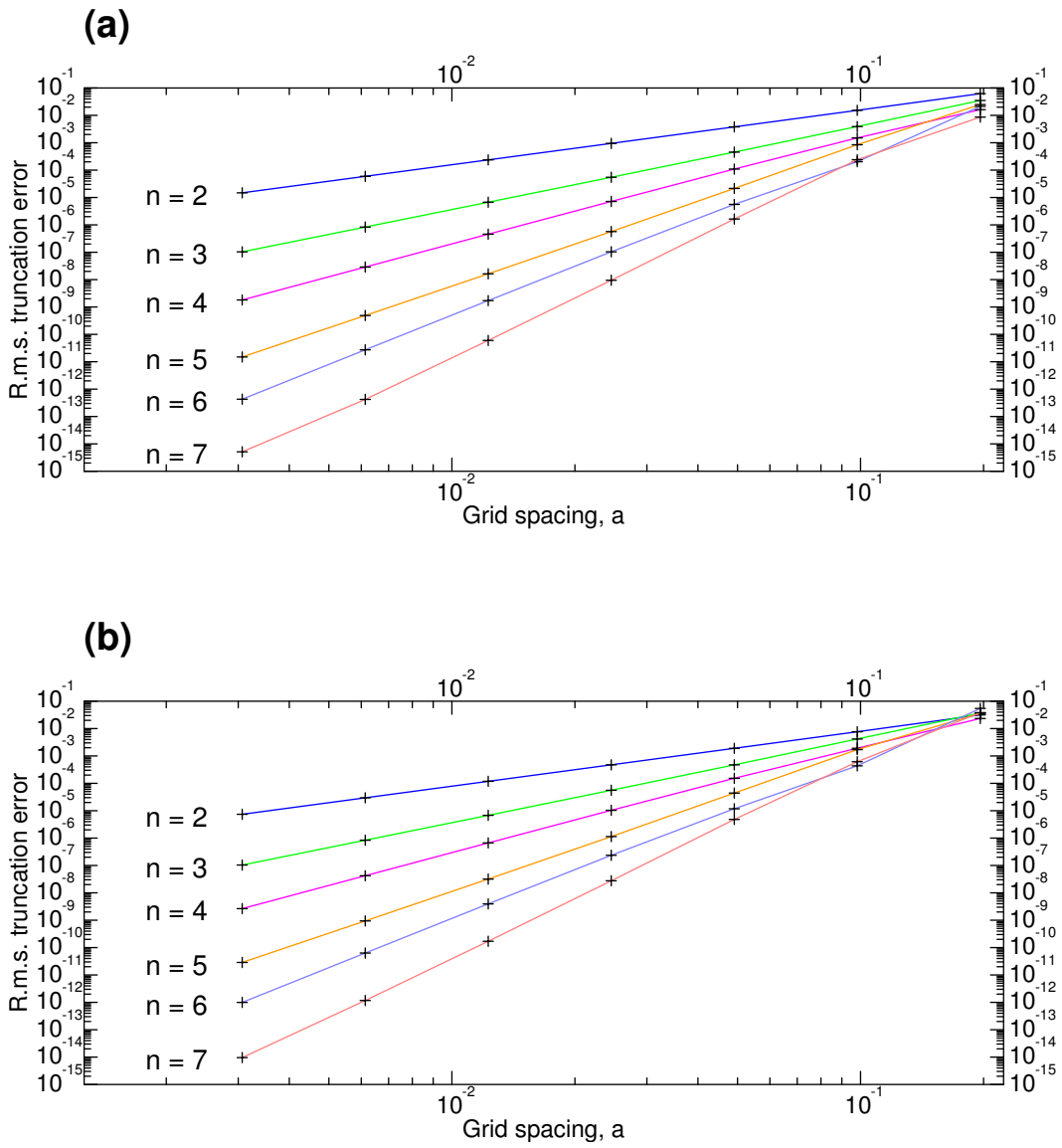

Figure 1. Curves showing the root mean square (r.m.s.) error in the numerical evaluations of integrals of smooth curves along a line segment using different orders of end correction terms, n, and different grid resolutions, a: (a) the extended trapezoidal methods; (b) the extended midpoint methods. The orders of accuracy, n, are in each case equal to the asymptotic slopes of the curves plotted.

In order to illustrate the beneficial effects of these extended schemes' correction terms, we take a test line segment to be the interval, $z \in [0, \pi]$, and form smooth random fields over this interval by setting the coefficients of superimposed terms $\cos(mz)$ and $\sin(mz)$ to unit-variance Gaussian random numbers for $m \leq 7$. The interval is resolved by grids with $a = \pi/16, a = \pi/32, \ldots, a = \pi/1024$ and the different extended schemes are tested for each of these grids and for each order of correction. The root mean square errors of the integral in each case are accumulated over ten separate random realizations (to reduce sampling excursions) and

the results are displayed in a pair of sets of log-log plots in Fig. 1. Fig. 1(a) shows the r.m.s. errors of the extended trapezoidal schemes; (b) the corresponding plots for the extended midpoint schemes. The slopes reflect the orders of accuracy achieved. Since, asymptotically for vanishing grid spaces, each of the graphs tends to a slope of n, this parameter gives the formal order of accuracy of the correction scheme. Note that, for relatively low resolution (the extreme right of the graphs), the higher orders of formal accuracy do *not* always guarantee actual reductions in r.m.s. errors in these examples.

3. Generalizing corrections to the Fibonacci grid

A Fibonacci grid may be characterized in several different ways. For a more complete description, we refer the reader to Swinbank and Purser (2005) as we shall only give a cursory summary here. Unlike most regular two-dimensional grids, where the structure is obtained as the intersections of two distinct families of regularly spaced coordinates, it is more natural to construct the points of a Fibonacci grid as a simple series of points regularly spaced (in azimuth, or longitude) along a shallow generative spiral. The radial extent of the spiral from the central pole is such that, for any cumulative azimuth, λ, the area $\mathcal{A}$ contained within the circle at this radial extent is directly proportional to λ. On a plane, where $\mathcal{A} = \pi r^2$ for a radius of r, the radius must therefore be in proportion to the square-root of the cumulative azimuth. Adopting j as the serial index of grid points spaced in azimuth or longitude by angle increments γ, then the plane polar coordinates $(r_j, \lambda_j)_a$ of the point labeled j must be:

$$(r_j, \lambda_j)_a = \left((ja/\pi)^{1/2}, \gamma j\right), \tag{3.1}$$

and hence the Cartesian coordinates for the grid with areal scale parameter, a, can be expressed as the set,

$$(\mathbf{x}_j)_{(a)} \equiv (a/\pi)^{1/2} \left[j^{1/2}\cos(j\gamma), j^{1/2}\sin(j\gamma)\right]. \tag{3.2}$$

In the case of a grid wrapped over a spherical surface, the area within the circle of co-latitude θ is, in Earth radius units, $\mathcal{A} = 4\pi \sin^2(\theta/2)$. Consequently, substituting co-latitude, θ_j for the r_j of the planar grid, we require that

$$\sin(\theta_j/2) = \frac{1}{2}(ja/\pi)^{1/2}, \tag{3.3}$$

in order to preserve the equal-area property of the grid with attributed area a per grid node.

While angle increments γ that are rational proportions of the full circle, 2π, always lead to undesirable clumping of grid points at sufficiently large radii, there are other, less obvious choices, where such clumping *never* occurs. The optimal angle in this respect is the 'golden angle' defined as the 'golden proportion' of 2π:

$$\gamma = 2\pi\sigma, \tag{3.4}$$

where this golden proportion, σ, is:

$$\sigma = \frac{2}{\sqrt{5}+1}. \tag{3.5}$$

The index j will take the values $j \in \{0,\ 1,\ \ldots\}$, when the grid contains the pole point, as is the case for the Fibonacci grid discussed in Hannay and Nye (2004). Alternatively, when j takes the values $j \in \{\frac{1}{2},\ \frac{3}{2},\ \ldots\}$, we obtain the version of the Fibonacci grid introduced by Swinbank and Purser (1999, 2005) for atmospheric modeling, which does not include the pole as a gridpoint. The areal quadratures over the first of these Fibonacci grids would, in the simplest case, weight the non-polar points equally by the amount a, and the pole points by a half of this measure, $a/2$; in this respect, the quadrature over this grid is perfectly analogous to the trapezoidal integration method. The simplest areal quadrature over the second, staggered version of these Fibonacci grids will assign equal weights a to *all* points, and is therefore perfectly analogous to the midpoint rule discussed in section 2.

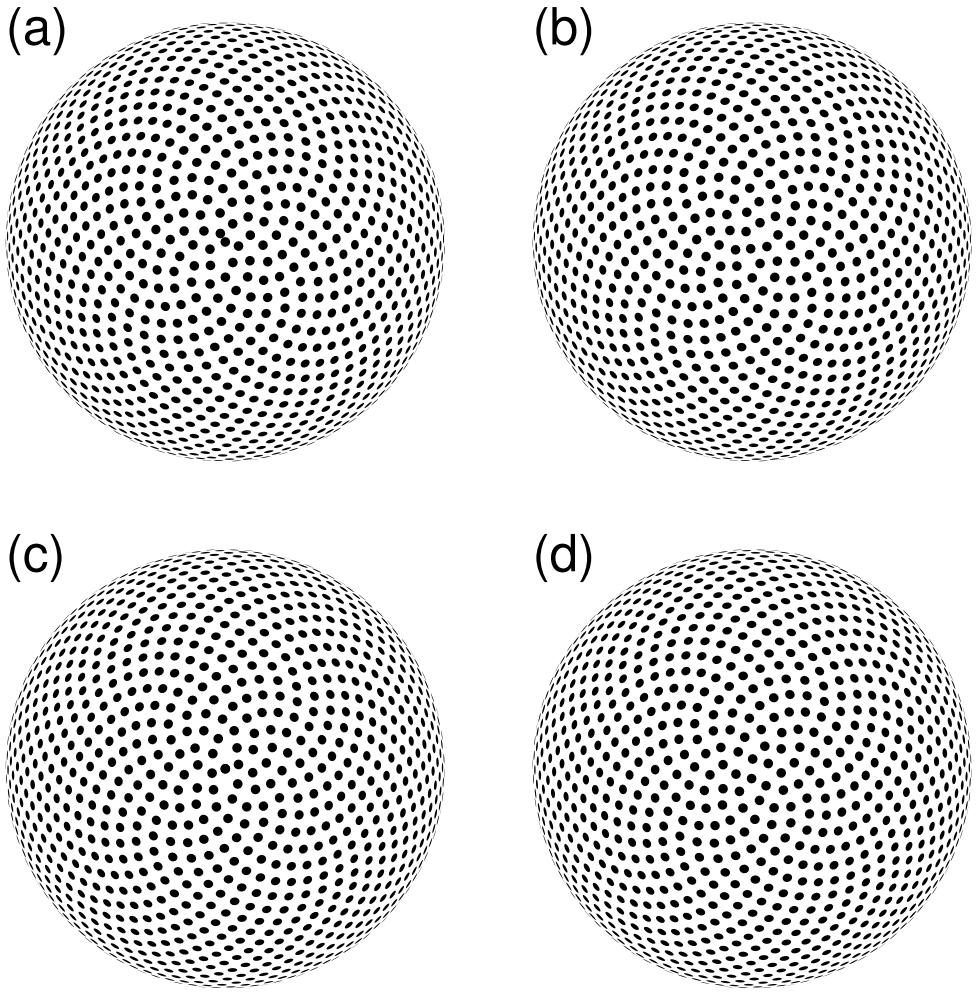

Figure 2. Views from above the pole of the patterns formed by the grid points of global Fibonacci grids whose points are either unstaggered or staggered with respect to the pole. (a) unstaggered single-spiral grid; (b) staggered single-spiral grid; (c) unstaggered two-spiral grid; (d) staggered two-spiral grid.

Since it is helpful to see what Fibonacci grids look like, Fig. 2 shows polar views of the patterns of grid points of four versions of the spherical Fibonacci grid, all with approximately 2000 points. Panels (a) and (b) show the basic Fibonacci grids that have a single generating spiral, respectively unstaggered and staggered with respect to the poles. Panels (c) and (d) show the analogous grids formed by placing two points per latitude (except possibly at the poles) and employing an alternative pair of generating spirals possessing twice the pitch. In these two-spiral grids, the longitudinal separation between points on the generating spirals is exactly a half that of the basic (one-spiral) Fibonacci grids of panels (a) and (b). Fig. 3a shows a view of the so-called Delaunay triangulation of the basic staggered grid shown in Fig. 2b. A Delaunay triangulation is one in which the circumcircle of each triangle contains no other grid points in its interior (Chynoweth and Sewell 1990). This triangulation gives the configuration of edges of the 3998-sided polyhedron formed as the convex-hull in three-dimensions of the points arranged on the sphere's surface. The dual 'Voronoi' configuration (Augenbaum and Peskin, 1985) shown in Fig. 3b connects with edges the centers of the circumcircles of those Delaunay triangles making finite contact. The uniformity of the areal coverage of the grid is visually apparent in these figures.

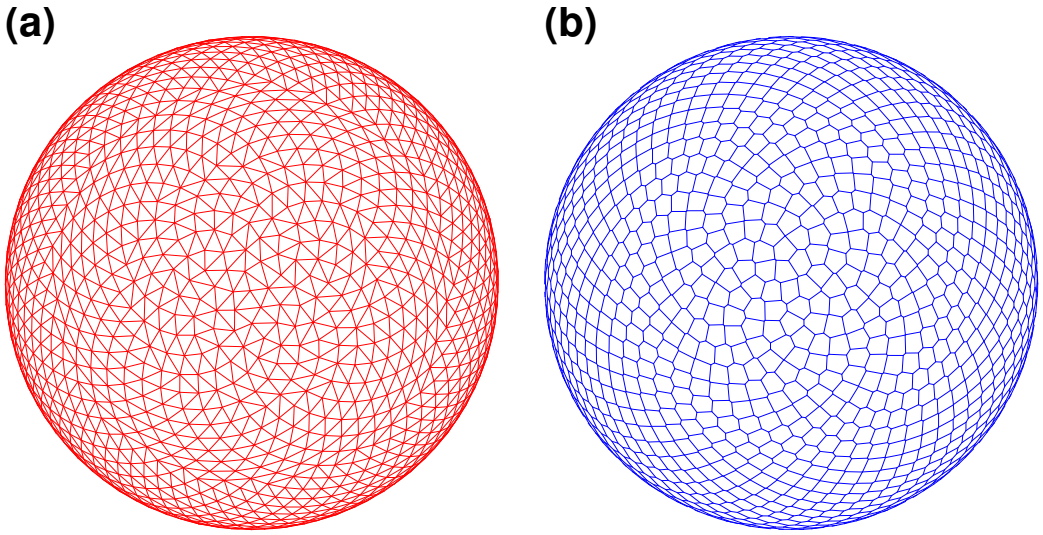

Figure 3. The global Fibonacci grid of 2001 points of Fig. 2b, but illustrated: (a) by its Delaunay triangulation; (b) the corresponding Voronoi tiling, showing the highly uniform areal distribution.

The aim of this section is to examine the steps required to effect correction terms to the weights at the 'ends' (i.e., immediately near the poles) that are analogous to those which, for the case of the line interval quadratures of section 2, are called the 'extended' trapezoidal and midpoint schemes. The complications we encounter for the Fibonacci grids are the fact that the quadratures are now two-dimensional, and the distribution of the Fibonacci points in each version of the grid cannot be separated into simple products of purely radial and azimuthal subdistributions. The sphericity is not a significant factor in the treatment of polar quadrature errors, so, for simplicity, we shall henceforth deal with the two planar forms of the Fibonacci

grid.

Naively, we should expect a numerical quadrature of a function f defined in the plane to be given by,

$$\int f\, ds \approx a \left\{ \frac{1}{2} f(r_0, \lambda_0) + \sum_{j=1}^{\infty} f(r_j, \lambda_j) \right\}, \tag{3.6}$$

for the version of the grid described in Hannay and Nye (2004) and by:

$$\int f\, ds \approx a \sum_{j=0}^{\infty} f(r_{j+\frac{1}{2}}, \lambda_{j+\frac{1}{2}}), \tag{3.7}$$

for the version of Swinbank and Purser (2005). In these formulae, we find that the errors caused by the end conditions scale in proportion to the *third* power of the *linear* grid scale, $\sqrt{a}$. Thus any correction formulae must achieve at least fourth-order accuracy to be worth applying.

Corresponding to what is achieved for the one-dimensional grids of section 2, the main idea of this section is to seek a minimal number $M(n)$ of the grid points at the polar extremes of the Fibonacci grid where additive modification to the weights by amounts aW_j^+ or $aW_{j+1/2}^-$ in formulae (3.6) or (3.7) respectively, for $j = 0, \ldots M(n) - 1$, leads in each case to a quadrature of formal order of accuracy $n > 3$.

It turns out that the required number $M(n)$ is given by

$$M(n) = (n-1)(n-2)/2, \tag{3.8}$$

as this is the number of independent coefficients of the general polynomial moment in $x = r\cos\lambda$ and $y = r\sin\lambda$ of degree $n-3$ which the modified quadratures need to be able to compute without error in order to attain the formal order of accuracy of n. We can systematically construct $M(n)$ polynomial test functions that span the space of polynomials up to the requisite degree, $n-3$ as indicated by the scheme of (3.9a)–(3.9c) below, where the polynomials are expressed as real and imaginary parts of generally complex functions of the polar variables, r and λ:

$$h_{0,0} = 1, \tag{3.9a}$$

$$h_{1,1} = r\exp(i\lambda), \tag{3.9b}$$

$$[h_{2,0},\ h_{2,2}] = \left[r^2,\ r^2\exp(2i\lambda)\right] \tag{3.9c}$$

and so on. The generic pattern gives

$$h_{p,q} \equiv r^p \exp(qi\lambda), \qquad p \geq q \geq 0, \qquad (p-q) \bmod 2 = 0. \tag{3.10}$$

Note that the successive rows of polynomials contained in these equations (3.9a)–(3.9c), and their continuation, combine to span the $M(n)$ degrees of freedom of all the polynomials up to the degree of those of the last row included. With $M(3) = 1$, the polynomials of degree-0 are just multiples of one, and the order of accuracy, $n = 3$ is already attained with the unmodified schemes. Thus the first nontrivial modification, required to give fourth-order quadratures, requires a modification to the weights of the three final points of the Fibonacci grids.

As before, we can regularize the test functions to keep their integrals and the discrete summations that approximate them finite. For example,

$$h_{p,q,\omega} \equiv \exp(-\omega\pi r^2) h_{p,q}, \tag{3.11}$$

and define the *principal value* of each *complex* error coefficient $\mathcal{E}^{\pm}_{p,q}(a) = \lim_{\omega\to 0} \mathcal{E}^{\pm}_{p,q,\omega}(a)$ as we did in section 2. With this convention understood, consider the terms that contribute to the error coefficient for generic test function, (3.11) in the unstaggered form of the Fibonacci grid.

$$\mathcal{E}^{+}_{p,q,\omega}(a) = a\left[\frac{1}{2}h_{p,q,\omega}(\mathbf{x}_0) + \sum_{j=1}^{\infty} h_{p,q,\omega}(\mathbf{x}_j)\right] - \int_{-\infty}^{\infty}\int_{-\infty}^{\infty} h_{p,q,\omega}(\mathbf{x})\, dx\, dy. \tag{3.12}$$

By symmetry, the integral vanishes unless $q = 0$, in which case this integral becomes real-valued and essentially one-dimensional:

$$\begin{aligned}\int_{-\infty}^{\infty} h_{p,0,\omega}(\mathbf{x})\, dx\, dy &= \int_0^{\infty} r^p\ \exp(-\omega\pi r^2)\, d(\pi r^2), \\ &= \pi^{-p/2}\int_0^{\infty} z^{p/2}\exp(-\omega z)\, dz.\end{aligned} \tag{3.13}$$

But in this case, we obtain (via a trivial change of variable in the integral):

$$\mathcal{E}^{+}_{p,q,\omega}(a) = \frac{a^{p/2+1}}{\pi^{p/2}}\left[\frac{1}{2}h_{p,0}(\mathbf{0}) + \sum_{j=1}^{\infty}(j)^{p/2}\exp(-\omega a j) - \int_0^{\infty} z^{p/2}\exp(-\omega a z)\, dz\right], \tag{3.14}$$

which, apart from the factor $1/(\pi^{p/2})$, is the same as the calculation in section 2 of the error coefficient, $\mathcal{E}^{+}_{p/2,\omega a}(a)$, for the trapezoidal rule. The calculations for $\mathcal{E}^{-}_{p,0,\omega}(a)$ similarly reduce to corresponding near-copies of the previous calculations, so that:

$$\mathcal{E}^{\pm}_{p,0,\omega}(a) = \frac{a^{p/2+1}}{\pi^{p/2}} E^{\pm}_{p/2,\omega a}. \tag{3.15}$$

Exploiting this coincidence, we shall scale the standardized error coefficients for the Fibonacci grids according to the definition

$$E^{\pm}_{p,q,\omega a} = \pi^{p/2}\mathcal{E}^{\pm}_{p,q,\omega}(1), \tag{3.16}$$

with the principal values defined by the limits:

$$E^{\pm}_{p,q} = \lim_{\omega\to 0} E^{\pm}_{p,q,\omega}. \tag{3.17}$$

In the cases where $q \neq 0$, the part involving the integral vanishes, as does the pole-point discrete evaluation in the unstaggered grid. The summation over non-polar Fibonacci grid points can be expressed as the equivalent integrals along the generative spirals involving the appropriate comb function. Defining:

$$Q_q(z) = \exp(2\pi i q\sigma z), \tag{3.18}$$

then, since when $z = \pi r^2$, the factorization,

$$h_{p,q}(r, \lambda) = \pi^{-p/2} f_{p/2}(z) Q_q(z) \tag{3.19}$$

becomes true at every grid point, we are able to express the standard error coefficients as integrals:

$$E^{\pm}_{p,q} = \int_{-\infty}^{\infty} C^{\pm}(z) f_{p/2}(z) Q_q(z)\, dz, \qquad q \neq 0. \tag{3.20}$$

The Fourier transform of Q_q is simply,

$$\tilde{Q}_q(k) = \delta(q\sigma + k), \tag{3.21}$$

as can be verified by substituting the $\tilde{Q}_q(k)$ into (2.5a) The formulae for the transform of $f_{p/2}$ given by (2.13) remain valid for half-integer values of $p/2$, so we may immediately obtain the $E^{\pm}_{p,q}$ for non-zero q as the evaluated convolutions:

$$\begin{aligned} E^{\pm}_{p,q} &= \tilde{C}^{\pm} * \tilde{f}_{p/2} * \tilde{Q}_q \Big|_{k=0}, \\ &= \sum_{m=-\infty}^{\infty} (\pm)^m \tilde{f}_{p/2}(m + q\sigma), \qquad q \neq 0. \end{aligned} \tag{3.22}$$

It is a simple matter to estimate the convergent summations from each of these two-sided complex series and to extract the individual error coefficients from their real and imaginary parts.

The first few of these moments for the unstaggered case are listed in Table 5 while those for the staggered form of the Fibonacci grid are given in Table 6. Owing to certain inherent symmetries, we find that several of the coefficients vanish.

TABLE 5. REAL AND IMAGINARY PARTS OF THE ERROR MOMENTS E^+ FOR THE FIRST FEW TEST POLYNOMIALS JOINTLY IN x AND y FOR THE FIBONACCI GRID UNSTAGGERED WITH RESPECT TO THE POLE.

AZIMUTHAL FUNCTION	RADIAL PROFILE				
	1	r	r^2	r^3	r^4
1	0.		−.8333333333E−1		0.
$\cos\lambda$		−.4061083458E+0		−.1484051532E+0	
$\sin\lambda$		−.9502485619E−1		0.7545644375E−1	
$\cos 2\lambda$			−.5479006077E+0		0.
$\sin 2\lambda$			0.		−.5980912825E+0
$\cos 3\lambda$				−.1195715249E+1	
$\sin 3\lambda$				0.1160062907E+1	
$\cos 4\lambda$					0.
$\sin 4\lambda$					−.2210942827E−1

Having computed the errors incurred in the application of (3.6) and (3.7) to the quadrature of the first few test polynomials, it is a relatively trivial task to adapt the procedure described in (2.21) to the present two-dimensional grids. This determines the weight correction coefficients, $W_{j,n}$, that are applied to the first $M(n) = (n-1)(n-2)/2$ points in order to achieve the intended order of accuracy, n. That is, we increment the actual weight of grid point j by the

TABLE 6. Real and imaginary parts of the error moments E^- for the first few test polynomials jointly in x and y for the Fibonacci grid staggered with respect to the pole.

azimuthal function	radial profile 1	r	r^2	r^3	r^4
1	0.		0.4166666667E−1		0.
$\cos\lambda$		0.8251824397E−1		0.7251031068E−1	
$\sin\lambda$		0.2195009067E+0		−.1312820553E+0	
$\cos 2\lambda$			0.4040048564E+0		0.
$\sin 2\lambda$			0.		0.6260646693E+0
$\cos 3\lambda$				−.1150027149E+1	
$\sin 3\lambda$				0.1175104534E+1	
$\cos 4\lambda$					0.
$\sin 4\lambda$					−.1274133923E+0

amount $aW_{j,n}$. These weights $W_{j,n}$ are listed in Table 7 for the first few Fibonacci grid points in the version unstaggered with respect to the pole, and in Table 8 for the first few points of the version staggered with respect to the pole. Thus, the quadrature formulae that improve upon the accuracies attained by (3.6) and by (3.7) are

$$\int f\,ds \approx a\left\{\frac{1}{2}f(r_0,\lambda_0)+\sum_{j=1}^{\infty}f(r_j,\lambda_j)+\sum_{j=0}^{M(n)-1}W_{j,n}f(r_j,\lambda_j)\right\}, \tag{3.23}$$

and

$$\int f\,ds \approx a\left\{\sum_{j=0}^{\infty}f(r_{j+\frac{1}{2}},\lambda_{j+\frac{1}{2}})+\sum_{j=0}^{M(n)-1}W_{j+\frac{1}{2},n}\,f(r_{j+\frac{1}{2}},\lambda_{j+\frac{1}{2}})\right\}, \tag{3.24}$$

respectively.

The new extended quadrature schemes have been tested at a large range of areal resolutions with smooth, statistically homogeneous random fields on the sphere (exactly analogous to the randon harmonic superpositions we used in the experiments to test the line-segment quadratures for Fig. 1). For the Fibonacci grids, the corresponding errors for the extended quadrature schemes are plotted in Fig. 4. Panel (a) shows the results for the grid unstaggered with respect to each pole; (b) shows the results for the staggered grid. These plots confirm the potential improvements that the modified quadratures can confer.

4. Discussion

We have shown how the analytic techniques of Fourier transforms and convolutions can be applied to derive the classical end-truncation errors of the trapezoidal and midpoint quadrature rules, and, with rather trivial adaptations, extended to give corresponding error coefficients for each of the *two-dimensional* Taylor series terms (here expressed as geometrically convenient combinations). Finding quadrature correction weights that nullify the principal errors is then a simple linear inversion which gives the correction weights we have been able to tabulate. We have tested these 'extended' schemes on random data fields and verified that they do indeed achieve the desired orders of formal accuracy. Regardless of the resolution of the Fibonacci

grid, and whether applied on the plane or on the sphere, the weights provided in Tables 7 and 8 will be generally applicable to the respectively pole-unstaggered and pole-staggered versions of the Fibonacci grid, and will tend to improve the accuracy of any calculations that involve the numerical integration of *smooth* scalar fields over the domain.

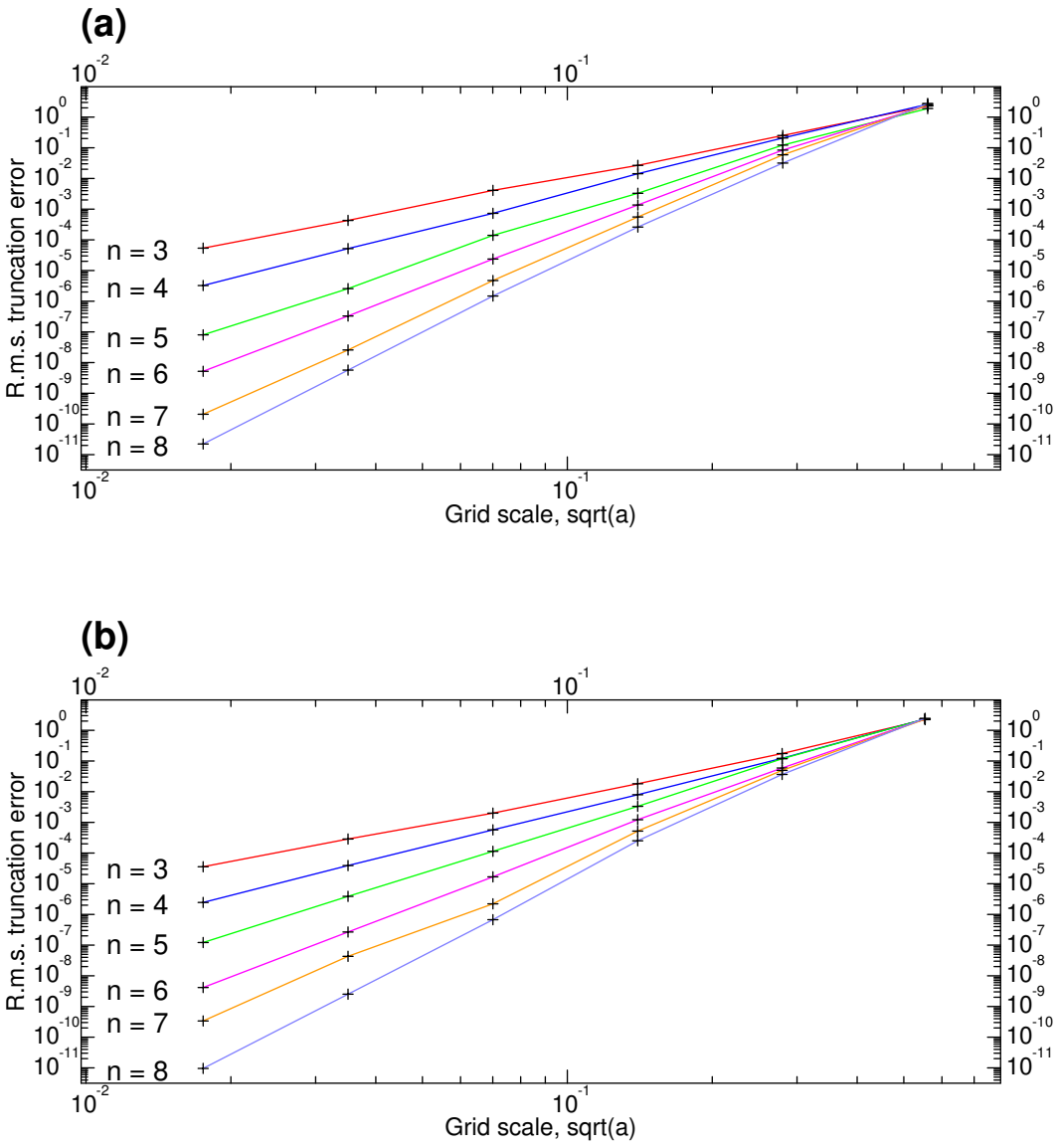

Figure 4. Curves showing the root mean square (r.m.s.) error in the numerical evaluations of integrals of smooth functions on a sphere using different orders n, of end correction terms at the polar ends of the spherical Fibonacci grid and different grid resolutions, $\sqrt{a}$ where a is the nominal average of the grid areas. (a) The case of a grid unstaggered with respect to the poles (analogous to the extended trapezoidal methods); (b) the case where the grid is staggered with respect to the poles (analogous to the extended midpoint methods). The orders of accuracy, n, are in each case roughly equal to the slopes of the curves plotted.

TABLE 7. POLAR CORRECTION WEIGHTS $W_{j,n}$ FOR QUADRATURE ON THE FIBONACCI GRID AT DIFFERENT ORDERS OF ACCURACY, n AND GRID POINT INDICES j FOR THE FIBONACCI GRID UNSTAGGERED WITH RESPECT TO THE POLE.

j	$n=4$	$n=5$	$n=6$	$n=7$	$n=8$
0	0.800418690E+0	0.310915476E+0	0.568438275E+0	0.657244435E+0	0.296940039E−1
1	−.586604663E+0	−.316216110E+0	−.426608268E+0	−.603124983E+0	−.706809266E−1
2	−.213814027E+0	−.150841849E+0	−.199697125E+0	−.305322425E+0	0.909210065E−1
3		0.295780220E−1	−.379570252E−1	−.972452390E−1	0.944007592E−2
4		0.203232293E−1	−.101639283E+0	0.912531890E−2	−.186644215E+0
5		0.106241231E+0	0.567689662E−1	0.134532221E+0	0.130936132E+0
6			−.521158691E−3	0.117788117E+0	−.445942852E−1
7			0.453087522E−1	0.722667885E−1	−.501923289E−1
8			0.312768870E−1	0.755747621E−1	0.766868111E−1
9			0.646299797E−1	0.514332290E−1	0.835946188E−1
10				−.118734600E−2	−.989447124E−1
11				−.243646954E−1	−.152590839E−1
12				−.279313890E−1	0.808294502E−1
13				−.376880128E−1	−.387472676E−1
14				−.211007808E−1	−.103584032E−1
15					0.407239290E−1
16					−.103457332E−1
17					−.226265956E−1
18					0.182713252E−1
29					0.105929584E−1
20					−.232967600E−1

Swinbank and Purser (1999) and Hannay and Nye (2004) discuss variants of the Fibonacci grid that put two or more points at the same latitude (see panels (c) and (d) of Fig. 2). Those grids with a higher symmetry around the pole are immune to the truncation errors associated with the $r\cos\lambda$ and $r\sin\lambda$ components that we see in Tables 5 and 6. Hence, without any modification, these alternative grids, while perhaps marginally less homogeneous near the poles, must nevertheless enjoy an order of accuracy advantage relative to the two 'basic' single-spiral Fibonacci grids we have restricted attention to in the present note. However, application of same kinds of methods we have illustrated here for the basic Fibonacci grids clearly also apply, with very minor adaptation, to the tasks, first, of evaluating the generalized 'Euler-Maclaurin' error coefficients for the more general multi-spiral grids and, second, of formulating appropriate correction weights that permit the modified quadrature schemes for these grids to attain a higher formal order of accuracy. Correction coefficients have been generated and validated for the first few multispiral grids unstaggered and staggered with respect to the pole but, for brevity, are not included in the present note.

We should not deceive ourselves into believing that a large n in the above schemes automatically imply a smaller truncation in absolute terms; if the function integrated has significant structure at scales barely resolved by the grid, the large excursions in the effective weights implied by the high-order correction terms can back-fire and produce *larger* truncation errors. For this reason, it is advisable to test the proposed schemes carefully on gridded fields typical of those whose surface integrations are required. For climate studies, the Fibonacci grid probably provides the most uniform areal coverage possible, which is very helpful to sub-grid-scale parametrization schemes which can be sensitive to grid scale. The proposed quadrature

TABLE 8. POLAR CORRECTION WEIGHTS $W_{j,n}$ FOR QUADRATURE ON THE FIBONACCI GRID AT DIFFERENT ORDERS OF ACCURACY, n AND GRID POINT INDICES j FOR THE FIBONACCI GRID STAGGERED WITH RESPECT TO THE POLE.

$2j$	$n=4$	$n=5$	$n=6$	$n=7$	$n=8$
1	−.193747070E+0	0.699316489E−1	0.399935447E−1	−.477857539E−1	−.427177031E−1
3	0.619037197E−1	−.870589557E−1	0.694418667E−3	0.314792150E−1	0.127406663E+0
5	0.131843350E+0	0.174012847E−1	0.503204456E−1	0.332498594E−1	0.432503010E−1
7		−.484261507E−1	−.149935663E+0	−.301202892E−1	−.164732017E+0
9		0.848926923E−1	0.704769902E−1	0.936104999E−1	0.348744171E−1
11		−.367405195E−1	−.604117603E−1	−.222062185E−1	−.194895490E−2
13			0.216633342E−1	−.573976372E−1	−.670350439E−1
15			−.550811131E−2	0.201619607E−1	0.269027409E−1
17			0.588285858E−1	0.922198439E−2	0.893320543E−1
19			−.261217843E−1	−.339519964E−1	−.480837032E−1
21				−.136814797E−1	−.474684631E−1
23				0.323300204E−2	0.534629002E−1
25				−.171525454E−1	−.131252222E−2
27				0.932071287E−2	−.209131602E−1
29				0.220186859E−1	0.268212158E−1
31					0.865703768E−2
33					−.193906755E−1
35					0.642500168E−2
37					0.151131479E−1
39					−.115725370E−1
41					−.707069964E−2

schemes allow the achievement of high-order accuracy without making any adjustments to the grid locations that would spoil the desirable homogeneous characteristics that these grids enjoy.

REFERENCES

Abramowitz, M., and I. A. Stegun 1965 *Handbook of Mathematical Functions*, Dover, New York. 1046 pp.

Augenbaum, J. M., and C. S. Peskin 1985 On the construction of the Voronoi mesh on a sphere. *J. Comput. Phys.,* **14,** 177–192.

Butcher, J. C. 1987 *The Numerical Analysis of Ordinary Differential Equations.* John Wiley, New York. 512 pp.

Chynoweth, S., and M. J. Sewell 1990 Mesh duality and Legendre duality. *Proc. Roy. Soc. London,* **A428,** 351–377.

Gear, C. W. 1971 *Numerical Initial Value Problems in Ordinary Differential Equations* Prentice-Hall, Englewood Cliffs, New Jersey, 253 pp.

Hannay, J. H., and J. F. Nye 2004 Fibonacci numerical integration on a sphere, *J. Phys. A,***37,** 11591–11601

Henrici, P. 1964 *Elements of Numerical Analysis*, Wiley, New York. 336 pp.

Press, W. H., S. A. Teukolsky, and W. T. Vetterling, B. P. Flannery 1992 *Fortran Numerical Recipes, Second Ed.* Cambridge University Press, 1486 pp.

Scheid, F. 1968 *Theory and problems of Numerical Analysis*, Schaum's Outline Series. McGraw-Hill, New York. 422 pp.

Swinbank, R., and R. J. Purser 1999 Fibonacci grids. *Preprint, AMS 13th Conference on Numerical Weather Prediction, Denver, 13–17 Sep. 1999*, pp. 125–128.

Swinbank, R., and R. J. Purser 2005 Fibonacci grids; A novel approach to atmospheric modeling. *Quart. J. Royal Meteor. Soc* (To appear. Preprint available as Met Office Forecasting Research Technical Report 468).